Simulation of Return Flow Generating Point in Uniform Hillslope with Variably Saturated Flows

O DEB Sanjit Kumar MIYAZAKI Tsuyoshi MIZOGUCHI Masaru IMOTO Hiromi

1. INTRODUCTION

Densely-packed traffic pan in hillslope unsaturated soils restricts downward water movement during prolonged rainfall episodes, and thereby leading to development of perched saturated zone and downslope saturated flow ensues. Saturation advances to surface, producing overland seepage as return flow, and preventing entry of further rainfall onto saturated area, which runs off directly. Potential for such saturation is therefore related to intersection of perched water table (PWT) and slope topography attributed to return flow, defining as return flow generating point (RFGP). The purpose of this study is to simulate RFGP.

2. GOVERNING EQUATIONS AND SIMULATION TECHNIQUE

The continuity equation of mass conservation for two dimensional water flow,

$$\frac{\partial \theta}{\partial t} = -\left(\frac{\partial q_z}{\partial z} + \frac{\partial q_x}{\partial x} \right) \tag{1}$$

q_x and q_z are fluxes in x and z axes, respectively; θ is soil water content. Assuming that soil is isotropic, q_x and q_z are defined based on Darcy's law,

$$q_x = -K\left(\frac{\partial \psi}{\partial x} - \sin \alpha \right); \; q_z = -K\left(\frac{\partial \psi}{\partial z} + \cos \alpha \right) \tag{2}$$

α is slope inclination, and $K\,(F, \psi)$ is unsaturated hydraulic conductivity (function of matric head ψ and specific geologic formation or soil type F). Substituting Eq.(2) into Eq.(1), Richards' equation of variably saturated flow for sloped porous media (**Fig.1**),

$$C\frac{\partial \psi}{\partial t} = \frac{\partial}{\partial z}\left(K \frac{\partial \psi}{\partial z} + K \cos \alpha \right) +$$
$$\frac{\partial}{\partial x}\left(K \frac{\partial \psi}{\partial x} - K \sin \alpha \right) \tag{3}$$

$C\,(F, \psi)$ is specific water capacity. For steady state flow, time-dependent $C\partial\psi/\partial t$ equals to zero in Eq.(3). Boundary conditions are either of flux type (Neumann) or fixed head type (Dirichlet).

(1) Boundary AB; infiltration and dynamic boundary condition switching between seepage and atmospheric:

$$AA': -K\left(\frac{\partial \psi}{\partial z} + \cos \alpha \right) = r \cos \alpha; \; z = D; \; 0 \le x \le L_r \tag{4a}$$

A'B: $\psi = 0$; $z = D$; $L_r \le x \le L_s$ (4b)

(2) Boundary BC (symmetry condition without incised stream at downslope), DC (traffic pan, conductivity

contrast across this boundary is large enough and very small contributions to flow system that occur below it), and AD (upslope divide); no flow boundaries:

$$BC: \frac{\partial \psi}{\partial x} - \sin \alpha = 0; \; x = L(L_r + L_s); \; 0 \le z \le D \tag{4c}$$

$$DC: \frac{\partial \psi}{\partial z} + \cos \alpha = 0; \; z = 0; \; 0 \le x \le L \tag{4d}$$

$$AD: \frac{\partial \psi}{\partial x} - \sin \alpha = 0; \; x = 0; \; 0 \le z \le D \tag{4e}$$

Initial condition (IC) in the flow region is given by,

$$\psi(x, y, t) = \psi_0(x, z) \quad \text{at} \quad t = 0 \tag{4f}$$

L_s is length of surface saturation. Boundary condition to apply along AB of **Fig.1** is unknown a priori since value of L_s is part of the solution. Water exfiltrated or rain (r) falling directly on L_s is removed from surface and must account for in mass balance. Surface runoff routing is not important as saturation proceeds upward from below above underlying traffic pan ($r < K_{s1}$).
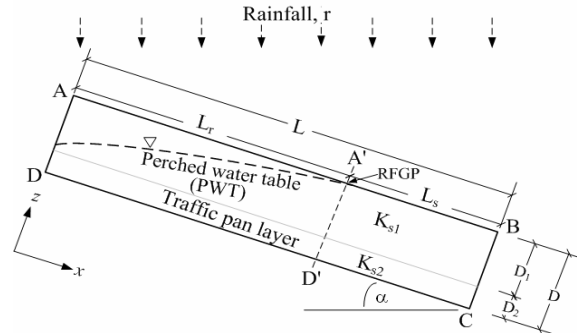
Fig.1. Definition sketch of RFGP and boundary conditions for the model hillslope.

Soil water retention behaviors and conductivity functions are described by either van Genuchten-Mualem (VGM) or VGM with air-entry ψ of *-2cm*:

$$\theta(\psi) = \theta_r + \frac{\theta_s - \theta_r}{[1 + |\alpha_v \psi|^n]^m} \quad \psi < 0$$

$$= \theta_s \quad \psi \ge 0 \tag{5a}$$

$$K(\psi) = K_s S_e^l [1 - (1 - S_e^{1/m})^m]^2 \quad n > 1 \tag{5b}$$

$Se\,[= (\theta-\theta_r)/(\theta_s-\theta_r)]$ is effective saturation; θ_r and θ_s are residual and saturated water content; α_v is inverse of air-entry value, n is pore-size distribution index, l (0.5) is pore-connectivity; and K_s is saturated conductivity. When air-entry value is set at *-2cm* in VGM, medium is considered constantly saturated at matric head below *2cm*, providing numerical stability near saturation. Brooks-Corey model is also applied:

$$S_e = |\alpha_v \psi|^{-n}, \quad \psi < -1/\alpha_v \; ; \; S_e = 1, \quad \psi \geq -1/\alpha_v \quad (6a)$$

$$K(\psi) = K_s S_e^{2/n+l+2} \quad (l = 2.0) \quad (6b)$$

Modified **HYDRUS-2D** finite element simulation model is used to solve Eq. (3) at steady state for the specified initial and boundary conditions. The 100 cm × 20 cm hillslope domain was discretized into square finite element grids and 10 simulation runs were performed under 50, 80, 100, 125, and 150 mm h^{-1} for both 8º and 12º model hillslopes, respectively (designated as SR1, SR2, and so forth).

3. ANALYTICAL CONSIDERATIONS

After prolonged rain, subsurface flux (q) is dominantly through saturated zone and PWT gradient is equal to α (**Fig.1**). PWT coincides RFGP along slope that mass balance at RFGP (A'D') under steady state,

$$rL_r cos\alpha = qA \quad (7)$$

L_r is RFGP from upslope; A is saturated soil depth*;* and q is described by Eq.(2) of $\partial \Psi/\partial x$ being zero for q$_x$,

$$q_x = K_s \sin \alpha \quad (8)$$

Substituting Eq.(8) into Eq.(7) yields,

$$L_r = \frac{AK_s tan\alpha}{r} \quad (9)$$

Eq.(9) is used to estimate steady state L_r and numerical model results are relied upon for this purpose.

4. MODEL SLOPE EXPERIMENTS

Laboratory setup described by Deb et al. (2004) for 100 cm × 5 cm × 20 cm volcanic ash soil model slopes was used and 10 experimental runs (ER1, ER2, and so forth) for 8º and 12º slopes was performed.

5. RESULTS AND DISCUSSION

5.1 Evolution of Matric Potentials and PWT

Figs.2a-2b demonstrate matric potential profiles for experimental and simulation runs ER1 and SR1 of 8° slope under 80 mm h^{-1}, respectively. Similar pattern of evolution of PWT and closer L_r are observed for both profiles. However, higher flow fields prevail in simulated profile, which are obviously attributed to higher optimized K_{s1} (0.064~0.12 cm s^{-1}) than those typically seen in field (0.014~0.038 cm s^{-1}), but are, however, physically realistic for this idealized hillslope with high infiltration capacity. Perched zone is highly triggered with K$_s$ contrast between top and pan layers, while growth of saturation depends on rainfall rates.

5.2 RFGPs

Fig.3 shows simulated, observed, and analytically-calculated L_r for 8° slope. Compared to simulated and observed values, analytical shows less L_r, indicating more slope saturation. In Eq.(9), PWT gradient above underlying traffic pan equals to α at RFGP. Since flow in saturated zone is proportional to PWT gradient, downslope fluxes for simulations or experiments seems much higher than that assumed in Eq.(9) because of continuous upslope flux additions. L_r decreases with higher r, i.e., saturation increases.

5.3 Hydraulic Models on Dynamics of PWT

Applications of VGM, VGM (*-2cm*) or Brooks-Corey in simulations would not influence significantly on PWT evolution. However, saturation appears earlier and faster for VGM (*-2cm*) and Brooks-Corey such that problem minimizes non-linearity in conductivity function near saturation. Other parameters ($n, \alpha, \theta_s, \theta_r$) influence to a smaller extent.

6. CONCLUSIONS

Simulated RFGPs by modified **HYDRUS-2D** are in good agreement with the observed and analytically-calculated values. Hence, for long uniform hillslope layered with traffic pan, prediction of RFGP relies on wherever PWT intersects slope surface during prolonged rainfalls. RFGP is triggered with K_s contrasts between hillslope top and traffic pan layers, and saturated growth is strongly with rainfall rates. Such RFGP is potential for soil erosion because of slope saturation formation and subsurface seepage.
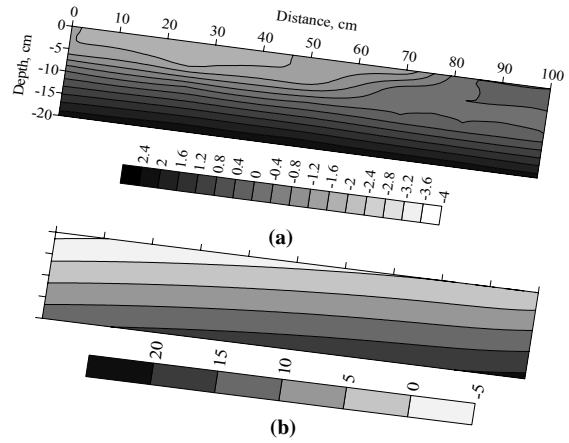
Fig.2. Demonstrative illustrations of steady state matric potential profiles (in cm) for 8° hillslope under 80 mm h^{-1} rainfall: (a) experimental run ER2, RFGP at 79.4 cm from upslope, and (b) simulation run SR2, RFGP at 76cm.
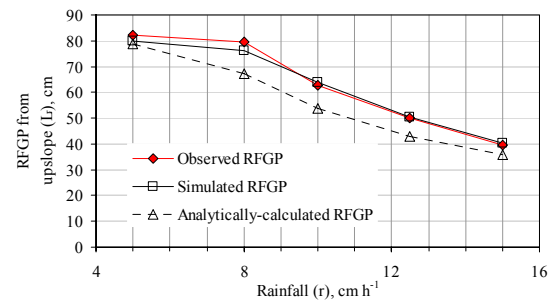
Fig.3. Demonstration of observed and simulated RFGPs for 8° hillslope experimental runs ER1, 2, 3, 4, 5 and simulation runs SR1, 2, 3, 4, 5 and 4 under steady rainfalls of 50, 80, 100, 125, and 150 mm h^{-1}, respectively. Analytically-calculated RFGPs using Eq.(9) for these rainfalls are also shown.

Reference
Deb, S. K., Miyazaki, T., Mizoguchi, M., and Imoto, H. (2004). Return flow generating point in unsaturated soils on a layered slope with traffic pan, *Abstracts, Proceedings of the Annual Meeting of the JSIDRE*, Sep 7~9, Sapporo, p.356-357.